

VI International Conference on Computational Methods for Coupled Problems in Science and Engineering
COUPLED PROBLEMS 2015
B. Schrefler, E. Oñate and M. Papadrakakis (Eds)

ADVANCED IMAGE PROCESSING METHODS FOR AUTOMATIC LIVER SEGMENTATION

PETR STRAKOS^{*}, MILAN JAROS[†], TOMAS KARASEK[†], TOMAS KOZUBEK[†],
PETR VAVRA^{††} AND TOMAS JONSZTA^{††}

^{*†} IT4I, VSB – Technical University of Ostrava
17. listopadu 15, 708 33 Ostrava
Czech Republic

^{*} e-mail: petr.strakos@vsb.cz

^{††} Faculty of Medicine - University of Ostrava
Syllabova 19, 703 00 Ostrava
Czech Republic

Key words: Image Processing, Automatic Segmentation, Liver, Computed Tomography, Magnetic Resonance Imaging.

Summary. This paper presents advanced methods of image segmentation suitable for automatic recognition of the human liver and its vessel system, but in general could be used to segment any organ or body tissue. The comparison of studied methods is being made in terms of segmentation quality and algorithm speed. The main criterion for quality evaluation of each selected method is the level of conformity between the automatically recognized boundary and the reference boundary specified by experienced user. For all the tests sequences of CT and MRI images were used.

1 INTRODUCTION

Nowadays digital image processing and analysis is extensively used in different areas of human activities. One of these fields is medicine, where the enormous amount of data has to be processed. In diagnostic medicine, radiologists use for example computed tomography (CT) or magnetic resonance imaging (MRI) to help diagnose diseases or to perform surgical procedures. Although those high-end technologies are very sophisticated and developed, there is still room for improvements especially in the area of post-processing. For example to plan the liver resection, surgeon will need an accurate 3D model of a liver with its vessel system. To visualize 3D data, volume rendering method is available and can be used directly. Disadvantage of this technique is that it does not provide any other information than 3D models for visualization itself. To obtain models for hemodynamics simulations or even models where volume of certain part of the model could be measured, methods of advanced image processing have to be used.

The keystone of the digital image processing methods is an image segmentation which works with pixel intensity levels. Segmentation methods like those based on regions (region growing) [1, 2, 3], thresholding (Otsu's methods) [1, 4], clustering (k-means clustering) [1, 5, 6] and others are available. Those techniques used solely without any further processing are

usually sufficient in cases where different parts of the image have significant differences in intensities of pixels like in cases of bones segmentation. The soft tissues like liver and its vessel system are much more challenging due to low contrast and direct influence of other organs which have the same intensity levels of the pixels.

In the paper three main image segmentation algorithms with other pre- and post-processing procedures are used for automatic image segmentation. Segmentation is used to recognize liver tissue and liver vessel system. The first segmentation algorithm is based on region growing [1, 2, 3], the second one works with multi Otsu's algorithm [1, 4] and the third one is based on k-means clustering [1, 5, 6]. In the paper comparison of above mentioned techniques and procedures in terms of segmentation quality and speed is provided. The main criterion for quality evaluation of each segmentation method is the level of conformity between the automatically recognized boundary and the reference boundary made by specialist. For all the tests sequences of CT and MRI images were used. Each modality of the input data had at least two different sources. One served as training data in the preparation phase and the other one was used for testing of the proposed methods. Combining three main segmentation algorithms and selected pre- and post-processing procedures five different methods for liver segmentation were used in total. Multi Otsu algorithm and k-means algorithm were then used to create two methods for segmentation of the liver vessel system.

Paper is organized in the following manner: in section 2 we present detailed description of each automatic segmentation method used for liver and the liver vessel system; in section 3 description of the image data selected for the tests is provided; section 4 describes evaluation method; in section 5 results of the evaluation are shown; section 6 discusses the results; section 7 brings the conclusion.

2 AUTOMATIC SEGMENTATION METHODS

In this section description of the main segmentation methods is provided in more detail. All necessary steps for pre- and post-processing of the data are also described.

Introduced methods are considered as automatic in case we know at least one point within the segmented object. In case of liver segmentation it is a point inside the liver. For segmentation of vessel system we have to define one point inside the vessel system. Methods for determination of such point or points are described in more details in [7, 8].

2.1 Region growing algorithm

In general region growing algorithm is one of the region based techniques. This algorithm partitions an image into regions that are similar according to a set of predefined criteria [1, 2, 3].

In our case we use a region growing algorithm that groups every pixel around the seed point to one group. To add new pixel to the group, intensity of that particular pixel is evaluated and it is added to the group only if its intensity does not exceed the mean intensity of the group more than the tolerance. The region is grown in 4-neighbourhood manner (north, south, east and west) around the seed pixel, while in total 8-neighbours are available around the pixel.

2.2 Multi Otsu algorithm

Multi Otsu algorithm [1, 4] uses multilevel thresholding to segment the image. It works with pixel intensity levels. Histogram of an image is divided into M classes. The number of classes is user defined parameter. To divide the histogram into M classes $M-1$ thresholds are necessary. Optimal threshold values are chosen in such a way that between-class variance is maximized. Every pixel in the image is then classified into one of the M classes based on the rule described in (1).

$$\begin{aligned}
 g(i, j) &= 1 \quad \text{for} \quad f(i, j) < T_1 \\
 &= 2 \quad \text{for} \quad T_1 \leq f(i, j) < T_2 \\
 &\vdots \quad \vdots \quad \quad \quad \vdots \\
 &= M \quad \text{for} \quad T_{M-1} \leq f(i, j)
 \end{aligned} \tag{1}$$

where $f(i, j)$ is image pixel and $g(i, j)$ is pixel after classification into one of the M classes.

2.3 K-means clustering

K-means clustering is image segmentation algorithm based on clustering. This algorithm partitions n pixels into k clusters, where k is integer value that holds $k < n$. K-means algorithm classifies pixels in an image into k number of clusters according to some similarity feature like grey level intensity of pixels and distance of pixel intensities from centroid pixel intensity [1, 5, 6]. The algorithm works in the following way:

- (i) Selection of k clusters (it is a user defined parameter)
- (ii) Calculation of the total number of image pixels N
- (iii) Random selection of k initial pixel intensity centroids μ_j
- (iv) Calculation of distances D_{ij} between pixel x_i and each centroid μ_j as in (2). Particular pixel x_i is then classified to cluster c_j to which centroid it has the smallest distance

$$D_{ij} = (x_i - \mu_j)^2 \tag{2}$$

where $i = 1 \div N$ and $j = 1 \div k$.

- (v) Re-calculation of centroid positions μ_j as a mean value from all pixel intensities which belong to cluster c_j .

$$\mu_j = \frac{1}{l_j} \sum_{i=1}^{l_j} x_i \tag{3}$$

where l_j is a number of pixels that belong to cluster c_j .

- (vi) Steps (iv) and (v) are repeated until classification of image pixels does not change or equivalently centroids do not move.

2.4 Pre-processing procedures

Before image segmentation could be performed images have to be pre-processed to reduce noise. Different noise reducing filters are available. In this paper adaptive Wiener filter was used for this purpose. Adaptive Wiener filter is based on statistics estimated from a local

neighborhood of each pixel [9].

Determination of necessary parameters for the three segmentation algorithms to run without further user intervention could be also considered as one of the steps of the pre-processing stage. In case of region growing algorithm optimal intensity tolerance was determined. In case of multi Otsu algorithm optimal number of dividing classes was determined and in case of k-means algorithm optimal number of segmenting clusters was determined. During the preparation phase series of ten images was segmented. Optimized parameter of each segmentation algorithm has varied in particular user defined band over each image and volumetric overlap error (VOE) (see section 4) was evaluated for every segmentation. Lowest sum of VOE values over all images specified the optimal value of the parameter to be used in the test phase. This part of pre-processing can be thus considered as a reference model for the segmentation. The reference model supplies necessary parameters so the segmentation of test images can run automatically.

2.5 Post-processing procedures

To obtain boundaries of segmented objects flooding of segmented regions is performed. This is the main post-processing operation. Extracted boundaries can then be approximated by closed cubic spline. This is the case of liver segmentation where such smoothing of the boundary suits the expected shape of the liver. In case of vessel system segmentation only area flooding with the boundary extraction without spline approximation was used.

For area flooding with boundary extraction we used modification of the basic 4-directional flood-fill algorithm [10]. Modification resides in marking the boundary pixel every time the flooding boundary is met and not only flooding the area without creating the boundary. User can also size the flooding element of square shape above the 1 pixel minimum. This modification is used to minimize the flooding of the areas with narrow connections to the main area. These areas usually occur in over-segmented images (more area is being segmented as part of the segmented object).

For the spline approximation we used periodic cubic spline [11] to smooth the segmented boundary of the liver.

Based on the specified post-processing procedures five different methods to segment the liver and two different methods to segment the vessel system have been evaluated in this paper. For liver segmentation it was:

- (i) Multi Otsu method with 8 or 5px flooding element (Multi Otsu 8(5)px flood)
- (ii) Multi Otsu method with 1px flooding element (Multi Otsu)
- (iii) K-means method with 8 or 5px flooding element (K-means 8(5)px flood)
- (iv) K-means method with 1px flooding element (K-means)
- (v) Region growing method (Region growing)

For vessel system segmentation it was:

- (i) Multi Otsu 1px flooding element without spline approximation (Multi Otsu)
- (ii) K-means 1px flooding element without spline approximation (K-means)

3 SELECTED IMAGE DATA

All evaluated methods were tested on two different modalities of the image data. We used data from the computed tomography (CT) and from the magnetic resonance imaging (MRI). All CT data had resolution of 512x512 pixels while MRI data had resolution 256x256 pixels. Publicly available DICOM database [12] was used as a source of data. Presented methods were used to segment the liver and the liver vessel system. Evaluated methods first proceeded through the preparation phase to establish settings which were then used in the test phase. Beside the different modalities, images from different patients were used as well. In preparation phase methods worked with series of ten images while the test phase performed on two images. Images in preparation phase always differ from those in the test phase. In Figure 1 example of two different modalities of the image data is shown.

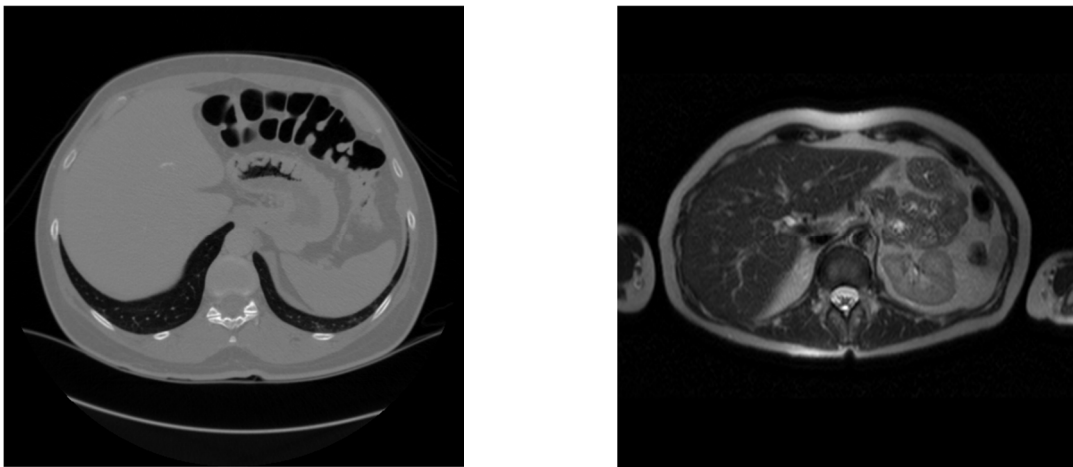


Figure 1: Example of the CT (left) and MRI (right) modality of the used image data

4 EVALUATION METHOD

Comparison of presented segmentation algorithms is based on computational time and segmentation quality.

Since each method ran in the preparation phase to establish important setting values which are then used in the subsequent test phase, two different runtime values were measured. First was the preparation phase runtime and the second was the test phase runtime.

Concerning the segmentation quality, several metrics are available [13, 14] which compare the segmentations with the manually segmented reference made by trained specialist. In this paper we use two metrics based on volumetric overlap. It is volumetric overlap error (VOE) and relative volume difference (RVD). As the main criterion for quality evaluation of each selected technique VOE is used. In section 5 where results are presented we use the mean VOE of two test images for the quality evaluation.

4.1 Volumetric overlap error

The volumetric overlap error (VOE) is given in percent and it calculates the error between two sets of pixels A and B as described in (4).

$$VOE = 100 \cdot \left(1 - \frac{|A \cap B|}{|A \cup B|} \right) \quad (4)$$

One of the pixel sets stands for the reference and the other one for the segmented set. Which set is which, whether A or B, does not matter as we calculate union and intersection between the sets. The 0 value of the volumetric overlap error means that there is a perfect match between the sets A and B. Value of 100 means that the pixel sets A and B do not overlap at all. The reason why this metric was used is that it is one of the most popular method for evaluation of the segmentation accuracy.

4.2 Relative volume difference

The relative volume difference (RVD) is also given in percent and it is calculated between two sets of pixels A and B by the equation (5).

$$RVD = 100 \cdot \left(\frac{|A| - |B|}{|B|} \right), \quad (5)$$

In equation (5) A stands for the segmented pixel set and B stands for the reference pixel set. The 0 value of equation (5) means both pixel sets have the same volume and in this sense they are identical. It has to be noted that this does not imply that A and B are identical, or overlap with each other. This is the drawback of the RVD method in comparison with VOE. On the other hand the RVD metric gives direct volumetric information. The RVD is a signed value and thus it also gives a good insight whether the method tends to over- or under estimate total volume. This is the main reason why RVD metric was used in this paper.

5 RESULTS

As mentioned earlier, tests were performed on two different images in each modality (CT and MRI) for liver segmentation and also on two images in each modality for vessel system segmentation. Results in Table 1 show numerical values for CT vessels segmentation. Images after segmentation are depicted in Figure 2. In Table 2 and Figure 3 results of CT liver segmentation are provided. Results for MRI modality are listed in Table 3 and Figure 4 in case of vessel segmentation. Results for MRI liver segmentation are listed in Table 4 and Figure 5. All results were obtained on PC with Intel Core i3, 1.9 GHz, with 4GB of RAM and MATLAB R2014a.

Table 1: Vessel segmentation results on two test CT images for evaluated methods. Mean VOE value calculated as mean from VOE values on each image.

	Prep. Runtime (~100 iterations) [s]	Runtime Image 1 [s]	VOE Image 1 [%]	RVD Image 1 [%]	Runtime Image 2 [s]	VOE Image 2 [%]	RVD Image 2 [%]	Mean VOE [%]
K-means	1174	6.1	57.959	11.640	5.3	62.014	7.931	59.987
Multi Otsu	28	2.9	58.576	-14.768	2.3	65.825	-27.500	62.201

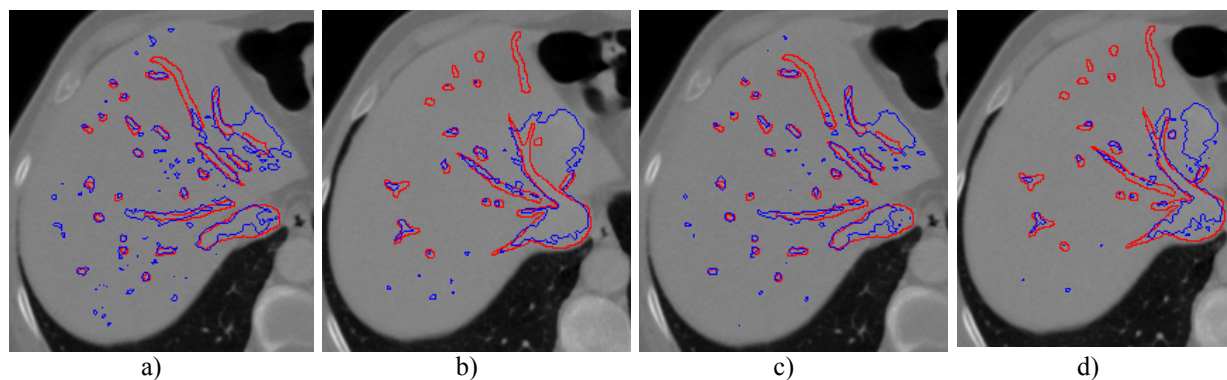


Figure 2: Vessel segmentation results on two CT test images for evaluated methods. Red line is reference, blue line is segmentation. a) K-means, image 1; b) K-means, image 2; c) Multi Otsu, image 1; d) Multi Otsu, image 2

Table 2: Liver segmentation results on two test CT images for evaluated methods. Mean VOE value calculated as mean from VOE values on each image.

	Prep. Runtime (~100 iterations) [s]	Runtime Image 1 [s]	VOE Image 1 [%]	RVD Image 1 [%]	Runtime Image 2 [s]	VOE Image 2 [%]	RVD Image 2 [%]	Mean VOE [%]
Multi Otsu, (8px flood)	355	4.8	4.623	-2.966	3.9	4.937	2.158	4.780
K-means, (8px flood)	1190	10.5	4.860	-3.770	9.9	5.407	-2.162	5.134
K-means	1190	13.0	6.044	-2.077	12.5	7.811	7.765	6.928
Multi Otsu	355	5.0	6.959	3.131	5.4	7.943	7.912	7.451
Region growing	499	5.3	6.186	-5.675	5.7	9.613	-8.493	7.900

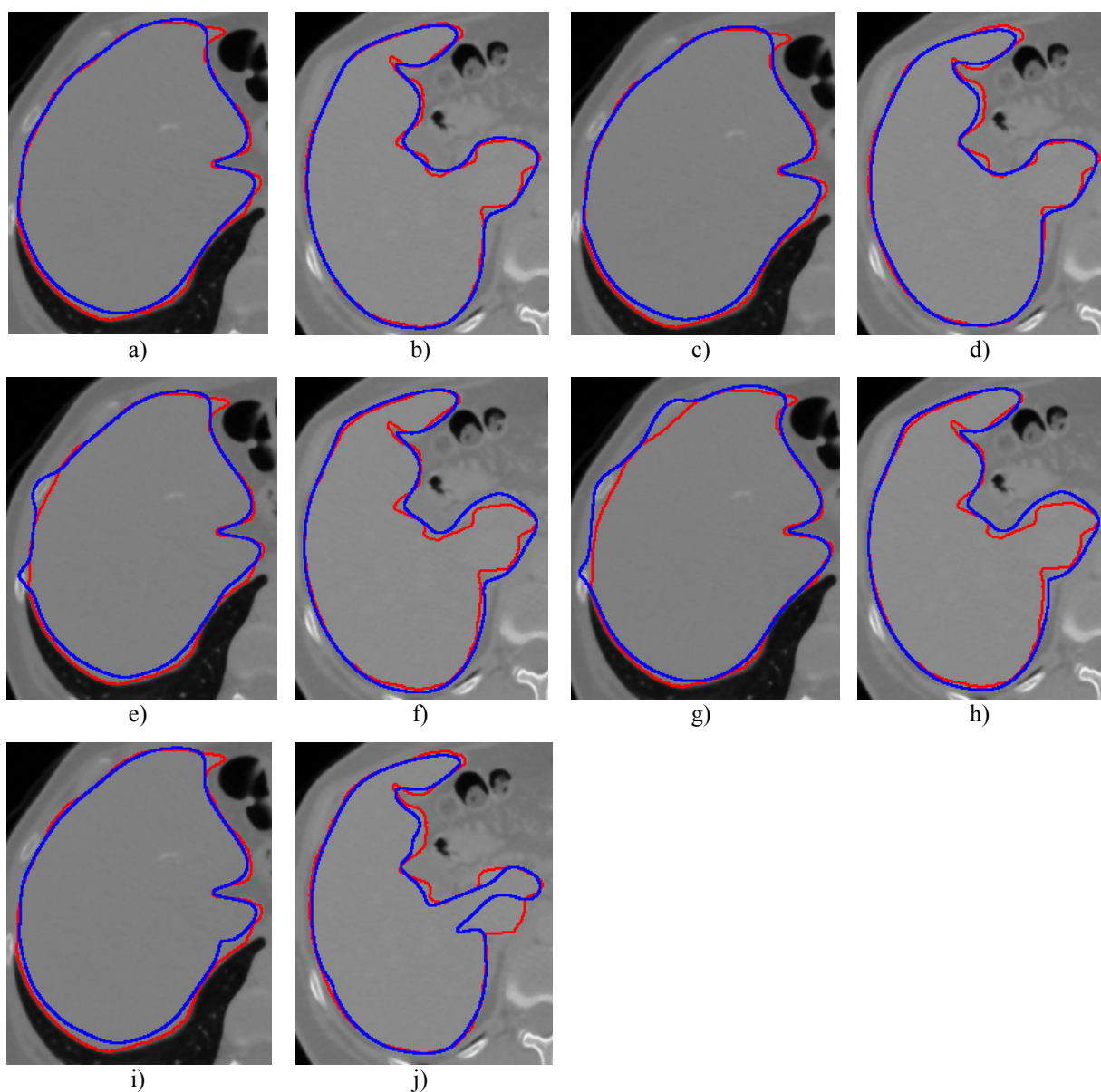


Figure 3: Liver segmentation results on two CT test images for evaluated methods. Red line is reference, blue line is segmentation. a) Multi Otsu (8px flood), image 1; b) Multi Otsu (8px flood), image 2; c) K-means (8px flood), image 1; d) K-means (8px flood), image 2; e) K-means, image 1; f) K-means, image 2; g) Multi Otsu, image 1; h) Multi Otsu, image 2; i) Region growing, image 1; j) Region growing, image 2

Table 3: Vessel segmentation results on two test MRI images for evaluated methods. Mean VOE value calculated as mean from VOE values on each image.

	Prep. Runtime (~100 iterations) [s]	Runtime Image 1 [s]	VOE Image 1 [%]	RVD Image 1 [%]	Runtime Image 2 [s]	VOE Image 2 [%]	RVD Image 2 [%]	Mean VOE [%]
Multi Otsu	12	1.2	78.681	-78.681	0.9	62.334	27.632	70.508
K-means	230	1.7	79.147	-79.147	0.9	62.589	25.804	70.868

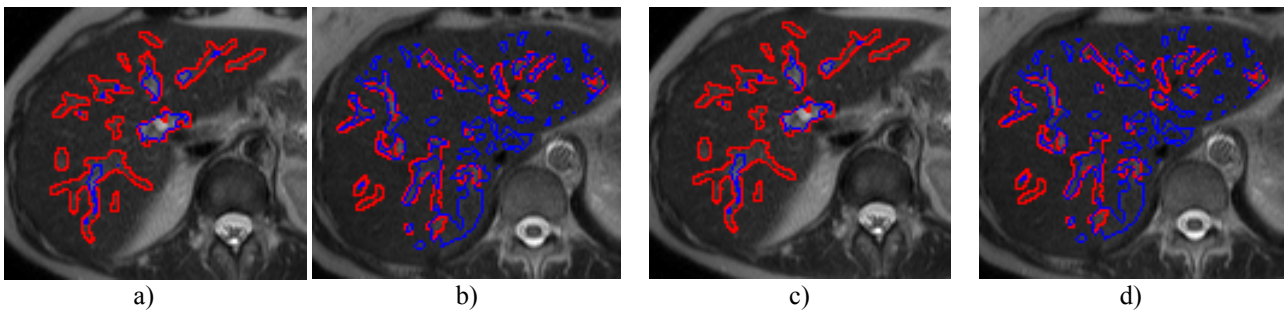


Figure 4: Vessel segmentation results on two MRI test images for evaluated methods. Red line is reference, blue line is segmentation. a) Multi Otsu, image 1; b) Multi Otsu, image 2; c) K-means, image 1; d) K-means, image 2

Table 4: Liver segmentation results on two test MRI images for evaluated methods. Mean VOE value calculated as mean from VOE values on each image.

	Prep. Runtime (~100 iterations) [s]	Runtime Image 1 [s]	VOE Image 1 [%]	RVD Image 1 [%]	Runtime Image 2 [s]	VOE Image 2 [%]	RVD Image 2 [%]	Mean VOE [%]
Multi Otsu, (5px flood)	72	1.3	11.538	2.035	1.3	18.585	3.350	15.062
K-means	321	3.1	17.940	-10.940	3.4	22.167	2.849	20.054
K-means, (5px flood)	321	2.6	32.661	-31.220	3.0	12.308	7.278	22.485
Region growing	96	1.9	26.490	-20.432	1.5	18.632	3.530	22.561
Multi Otsu	72	3.0	22.176	21.340	1.8	23.337	19.497	22.757

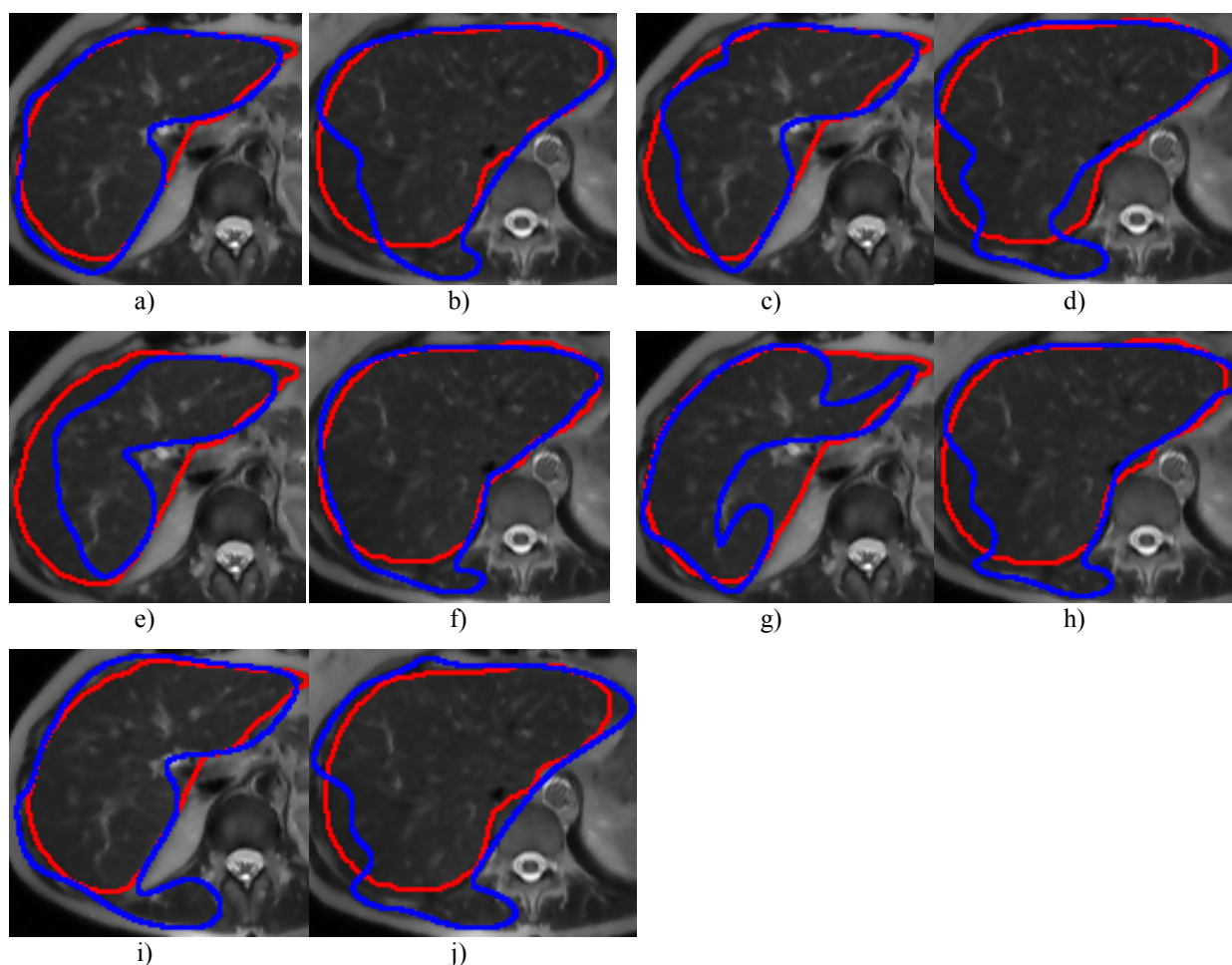


Figure 5: Liver segmentation results on two MRI test images for evaluated methods. Red line is reference, blue line is segmentation. a) Multi Otsu (5px flood), image 1; b) Multi Otsu (5px flood), image 2; c) K-means, image 1; d) K-means, image 2; e) K-means (5px flood), image 1; f) K-means (5px flood), image 2; g) Region growing, image 1; h) Region growing, image 2; i) Multi Otsu, image 1; j) Multi Otsu, image 2

6 DISCUSSION

By comparing automatic segmentation methods we could observe that the best results are obtained on CT modality when segmenting the liver tissue itself. CT modality brings two times higher resolution in comparison with MRI (see section 3). The lowest VOE value of 4.780 % is obtained by multi Otsu (8px flood) method. Possibility to restrict the flood fill algorithm to 8 pixels helps a lot since the plain method with 1 pixel flooding tends to over-segment. This is true also for k-means method in CT liver segmentation, see Table 2 and Figure 3. On the other hand region growing method tends to under-segment as can be seen in Table 2. This is why restriction of flood fill algorithm to higher pixel values has not been used for region growing method.

For the MRI modality of the liver tissue segmentation, multi Otsu (5px flood) is a best

performing method with VOE value of 15.062 %. Restriction of the flood fill algorithm does bring improvements only in the case of multi Otsu method which tends to over –segment in its non-restricted version.

From Table 1 and Table 3 can be observed that segmentation of the liver vessel system performs better on CT than MRI images. In case of CT the best VOE value of 59,987 % is produced by k-means method as shown in Table 1. In case of MRI images segmentation methods show almost identical results with VOE around 71 % as visible from Table 3.

Concerning the runtimes, long runtimes in preparation phase can be explained by high number of evaluations (10 evaluated images, each image processed approx. 10 times). Highest runtimes occur for k-means method. This is caused by the fact that k-means method execution time depends on initial setting of cluster centroids. If initial setting is far away from optimum, k-means takes long.

7 CONCLUSION

It has been shown that best performing segmentation method for liver segmentation is multi Otsu method with restriction of flood fill algorithm.

There is significant difference in segmentation quality when segmenting CT or MRI modality. This is due to two times less image information in MRI images in comparison to CT images. Therefore CT images appear as more suitable for the used segmentation techniques.

Segmentation of the liver vessel system does not show any particular advantage of any used methods. Slightly better results are obtained in case of CT data, which can be again explained by the fact that CT data contain two times more image information than MRI data. Problems in vessel segmentation are caused mainly by the presence of noise. It happens that small vessels simply disappear in the noise.

For a future work tested methods need to be effectively applied to the sequence of consecutive images covering the whole liver area. For segmentation of the liver vessel system different and more proper methods have to be searched since the presented methods are not very effective.

8 ACKNOWLEDGMENT

This paper has been elaborated in the framework of the project New creative teams in priorities of scientific research, reg. no. CZ.1.07/2.3.00/30.0055, supported by Operational Programme Education for Competitiveness and co-financed by the European Social Fund and the state budget of the Czech Republic.

REFERENCES

- [1] Sonka, M., Hlavac, V., Boyle, R. *Image Processing, Analysis and Machine Vision*. Thomson, (2006). ISBN 978-0-495-24428-7.
- [2] Neri, E., Caramella, D., Bartolozzi, C. *Image Processing in Radiology*. Springer, (2008). ISBN 978-3-540-49830-8.
- [3] Terry Y. *Insight into Images: Principles and Practice for Segmentation, Registration, and Image Analysis*. A K Peters/CRC Press, (2004), ISBN 978-1568812175.
- [4] Liao, P-S., Chung, P-C. A fast algorithm for multilevel thresholding, *Journal of*

- Information Science and Engineering* (2001) **17** (5):713-727.
- [5] Dass, R., Priyanka, Devi, S. Image Segmentation Techniques. *IJECT* (2012) **3** (1):2230-7109.
 - [6] Luo, S., Li, X., Li, J. Review on the Methods of Automatic Liver Segmentation from Abdominal Images. *Journal of Computer and Communications* (2014) **2**, pp 1-7. DOI: 10.4236/jcc.2014.22001.
 - [7] Ruskó L., Bekes G., Németh G., Fidrich M. Fully automatic liver segmentation for contrast- enhanced CT images. In: *Proceedings of MICCAI workshop on 3D segmentation in the clinic: a grand challenge*, pp 143–150.
 - [8] Juszczak, J., Piętka, E. Automatic generation of initial points for CT abdominal organ segmentation. *International Journal of Computer Assisted Radiology and Surgery* (2013) **8** (1 Supplement):263-336. DOI 10.1007/s11548-013-0880-0.
 - [9] Jin, F., Fieguth, P., Winger, L.; Jernigan, E. Adaptive Wiener filtering of noisy images and image sequences. *ICIP* (2003) **3**:1522-4880. DOI:10.1109/ICIP.2003.1247253.
 - [10] Flood fill, 2014. Available from: <http://en.wikipedia.org/wiki/Flood_fill>. [19 January 2015].
 - [11] Graham, N. Y. Smoothing With Periodic Cubic Splines. *Bell System Technical Journal* (1983) **62** (1), pp 101–110.
 - [12] DICOM files, 2014. Available from: <<http://www.osirix-viewer.com/datasets/>>. [16 January 2014].
 - [13] Heimann, T. et al. Comparison and evaluation of methods for liver segmentation from CT datasets. *IEEE Transactions on Medical Imaging* (2009) **28** (8):1251–1265.
 - [14] Mharib, A., Ramli, A., Mashohor, S., Mahmood, R. Survey on liver CT image segmentation methods. Springer Netherlands. In: *Artificial Intelligence Review* (2012) **37** (2):83-95. DOI: 10.1007/s10462-011-9220-3.